Hindawi
Advances in Materials Science and Engineering
Volume 2023, Article ID 9030449, 10 pages
https://doi.org/10.1155/2023/9030449

Research Article

Acoustic Emission Characteristics and Damage Evolution Analysis of Sandstone under Three-Point Bending Test

Tao Qin, Chen Jiang, Yanwei Duan, Yiwei Wang, and Chao Ju

Key Laboratory of Mining Engineering of Heilongjiang Province College, Heilongjiang University of Science and Technology, Harbin 150022, China

Correspondence should be addressed to Yanwei Duan; 1354070597@qq.com

Received 8 September 2022; Revised 2 October 2022; Accepted 5 October 2022; Published 1 February 2023

Academic Editor: Depeng Ma

In order to study the prevention of roadway roof bending, sinking, and breaking and the prevention of dynamic disasters such as the appearance of rock bursts, three-point bending experiments of sandstone under different spans were carried out. By using stress loading system and acoustic emission technology, the acoustic emission characteristic parameters of the sandstone fracture process were analyzed, the precursory information of rock bending fracture was explored, and the evolution law of sandstone damage based on acoustic emission characteristics was obtained. The results showed that according to the variation of acoustic emission ringing count, the load-time curve was divided into four typical stages: the first stage showed an overall increasing trend; the second stage showed an obvious increasing trend; the third stage showed obvious accelerated growth and the acoustic emission ringing count reached the maximum at the moment of rupture. In the fourth stage, the amplitude and frequency of the ringing count are large and high. With the increase in span, the cumulative ringing counts of AE decreased, and the rate of change gradually decreased. The fracture process of three-point bending sandstone can reflect the precursor information of rock fracture from time domain, frequency domain, and R value (ratio of cumulative acoustic emission ringing count to cumulative energy count). In time domain, the evolution characteristics of AE cumulative ringing count stage II can be used to predict the three-point bending fracture of sandstone. The peak frequency shows a linear increase after a spike and then an accelerated increase to a rupture, and the boundary point between the spike and the linear and nonlinear can be obtained. The decrease in R value can indicate that the main crack is growing in the specimen. According to the damage rate, the characteristics of the damage variables can be divided into five stages: stationary and low, gradually increasing, gradually decreasing, main crack coalescence, and complete fracture. With the increase in span, the fracture damage shows a decreasing trend. The residual damage fluctuates between 0.38 and 0.40 due to the difference in crack propagation trajectory. It has theoretical research value for revealing the internal mechanism of rock bending and fracture and has engineering guiding significance for mine pressure and rock strata control and dynamic disaster prevention.

1. Introduction

Underground mining causes the surrounding rock to be subjected to tensile, compressive, shear, or compound stresses, the root cause of rock damage is that the tensile or shear stresses reach their limits, and the roof bending and sinking fracture process is an important reason for the emergence of mine pressure and dynamic disasters [1–5]. Rock fracture has obvious local characteristics, and scholars have carried out a large number of studies related to the regional and overall damage laws of rock fracture, which have played an important role in understanding the mechanical characteristics and damage mechanisms in the process of rock damage. However, during the fracture and failure process of rock materials, the internal force and deformation process are very complex, and the deformation and damage characteristics of the internal and external zones of rock under different stress states will show obvious differences. The study of the internal microscopic change characteristics of rock during the instability and failure process has been one of the hot and difficult problems in rock mechanics research. In the study of rock fracture

mechanics, three-point bending specimens are simple to produce and easy to operate, and the results are representative, so the study of the fracture process of three-point bending has become particularly important [6–9].

For rock materials or rock-like materials, scholars have carried out a large number of three-point bending tests to study the fracture behavior of rock. Wei et al. [10] analyzed the fracture toughness and tensile strength characteristics of sandstone through a three-point bending test with an incision. Zuo et al. [11] studied the fracture characteristics and crack propagation law of granite under three-point bending through heat treatment. Through comparative analysis of the three-point bending test and the Brazilian splitting test, Heng et al. [12] studied the fracture propagation and evolution mechanism of shale. Lu et al. [13] studied the influence of the prefabricated crack method and prefabricated length on the fracture process through three-point bending test. Zhao et al. [14] studied the influence of particle size on the failure of rock-like materials based on bending test. Through numerical simulation, Han et al. [15] studied the influence of the strength properties of different bedding planes on rock failure during three-point bending.

A large number of scholars have carried out researches on the application of acoustic emission in rock fracture monitoring and achieved fruitful results. Yang [16] studied the microfracture behavior and acoustic emission characteristics of rock under hydraulic coupling through machine learning. Wang et al. [17] used acoustic emission technology to explain the law of granite crack growth by carrying out true triaxial tests on granite and building a cooperative prediction model for rock failure time. Liu et al. [18] carried out the Brazilian splitting test and used acoustic emission technology to explore the relationship between RA (the ratio of rise time to amplitude) and AF (average frequency) of acoustic emission characteristic parameters and crack failure mode. Li et al. [19] carried out a uniaxial loading test of coal and rock mass, used acoustic emission technology for monitoring, and analyzed the instability and failure process of coal and rock mass by analyzing acoustic emission waveform characteristics through the HHT method. Yang et al. [20] carried out triaxial unloading confining pressure experiments with different unloading rates and initial confining pressures and discussed the relationship between fractal characteristics of the AE time series of coal and rock mass and its instability and failure.

Based on the above research, this paper uses stress loading system and acoustic emission technology to carry out three-point bending experiments of sandstone with different spans, analyzes the acoustic emission characteristic parameters of the sandstone fracture process, explores the precursory information of rock bending and fracture, and obtains the sandstone damage evolution law based on acoustic emission characteristic representation. It is of great significance to study the prevention of bending and subsidence fractures of roadway roof and the prevention of dynamic disasters such as rock burst.

2. Introduction to the Three-Point Bending Test

2.1. Experimental Scheme. Dense and uniform sandstone specimens were selected and processed into rectangular specimens of 50 mm × 50 mm × 200 mm, and the six end faces of the specimens were polished by grinding machines, with the dimensional error of the specimens within ±0.3 mm and the verticality error less than 0.25°. The specimens were calibrated one by one by rock sample ultrasound, and specimens with similar wave speed were selected to reduce the influence of discrete sandstone specimens on the experimental results. Rubber bands were attached to the ends of both sides of the specimens to fix the acoustic emission sensor probes, and the damage evolution and precursor information of rock bending fracture at different span distances were obtained through the acoustic emission system for sandstone specimens, see Figure 1.

The sandstone three-point bending experiments were set up in five groups of tests with different lower pivot spans, the spans of the pivot points were set to 180 mm, 170 mm, 160 mm, 150 mm, and 140 mm, and three specimens were carried out in each group of experiments, as shown in Figure 2.

2.2. Experimental System. The experimental setup mainly includes stress loading system and acoustic emission system, see Figure 3.

① Applying vertical load to the specimen by TAW-500 microcomputer-controlled electro-hydraulic servo system, the experimental device load control accuracy is 0.001 kN, and displacement control accuracy is 0.001 mm.

② Application of SH-II acoustic emission system to monitor the acoustic emission signal of the loading process, the frequency measurement range is 1 kHz~3 MHz, the acoustic emission probe model is Nano30, the measurement threshold value is 40 dB under no-load condition, the sampling rate is 1 MSPS, and the waveform signal and characteristic parameters are collected in real time.

3. Analysis of Acoustic Emission Characteristics of Sandstone Fracture Process

Figure 4 shows the relationship between load time and acoustic emission ringing counts for different span spans, and the experiments were loaded with equal displacement, and time was positively correlated with displacement. The load-time curve is divided into four typical stages by the fluctuation of acoustic emission ringing count. At the initial loading to a certain load, there is an obvious concentration of ringing counts, which divides the first stage; with the increase of load, there is a second obvious concentration of ringing counts, which divides the second stage; at the peak moment, there is a third high concentration of ringing counts, which divides the third stage, after the peak is divided into the fourth stage. The rupture of the sandstone under the three-point bending condition is localized and random, so the acoustic emission in the first and second stages also has random sudden rise and aggregation. The auxiliary line added by the load-time curve found that the curve before the peak can be divided into two typical stages,

Figure 1: Specimen preparation.

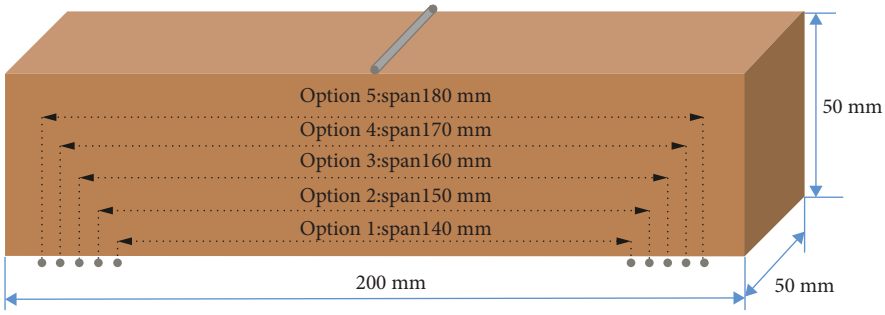

Figure 2: Layout of fulcrum span.

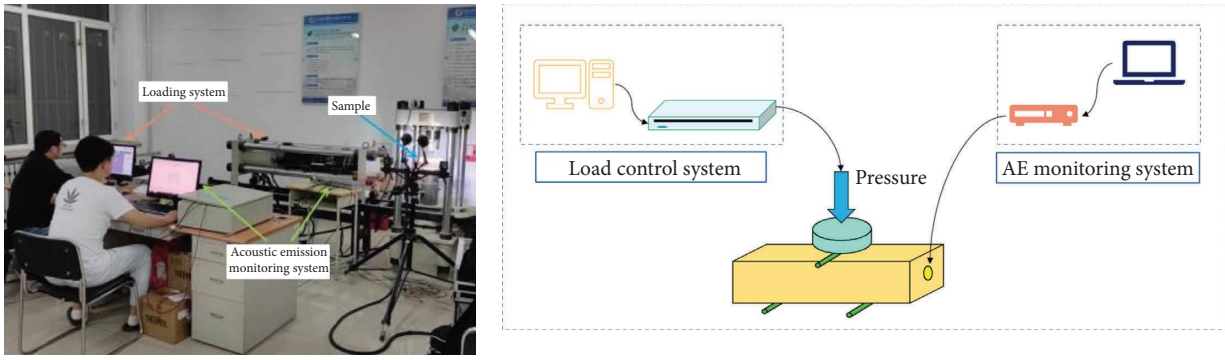

(a) (b)

Figure 3: Experimental system: (a) physical diagram of the experimental system and (b) schematic diagram of the experimental system.

linear elastic stage and nonlinear yielding stage, which indicates that the rock three-point bending experiment is essentially different from the typical uniaxial and triaxial compression deformation process, and the linear change in stage I makes it difficult to judge the compression-density stage by the load-time curve. The so-called neutral layer refers to the plane in the middle of the height direction of the rock sample. Accordingly, with the help of acoustic emission ringing count, fluctuation aggregation characteristics can determine the three-point bending compressive density stage.

The elasto-plastic cutoff point delineated by the load-time curve is not at the same location as the elasto-plastic cutoff point delineated by the acoustic emission ringing count, such as the span 180 mm and 150 mm curves tend to be earlier than the acoustic emission ringing count, and the span 160 mm curve tends to lag behind the acoustic emission ringing count. The consistency of the load-time curve fluctuation and peak moment with the acoustic emission ringing count indicates that the feedback of acoustic emission ringing count on the crack is significant, while the load-time curve trend responds to the characteristics of the sandstone as a whole, which is not sensitive to the change of microcracking.

The analysis of the acoustic emission ringing counts at each stage of different span spans revealed that stage I contains two cases, the acoustic emission signal was collected at the beginning of the experiment (no-load) (180 mm and 160 mm) and the acoustic emission signal was collected after the load was increased (170 mm, 150 mm, and 140 mm). With the increase of span distance, the overall trend of acoustic emission ringing count in stage I is increasing.

Stage II contains three cases, the acoustic emission ringing counts calmly vary slightly (span 170 mm, 150 mm, and 140 mm), slightly increase (span 180 mm), and more drastic fluctuating changes (span 160 mm). The first case is the change from disorderly to orderly microcracks under load, and the area near the rupture zone is more significant; the second case is a higher degree and number of primary crack adjustments, and

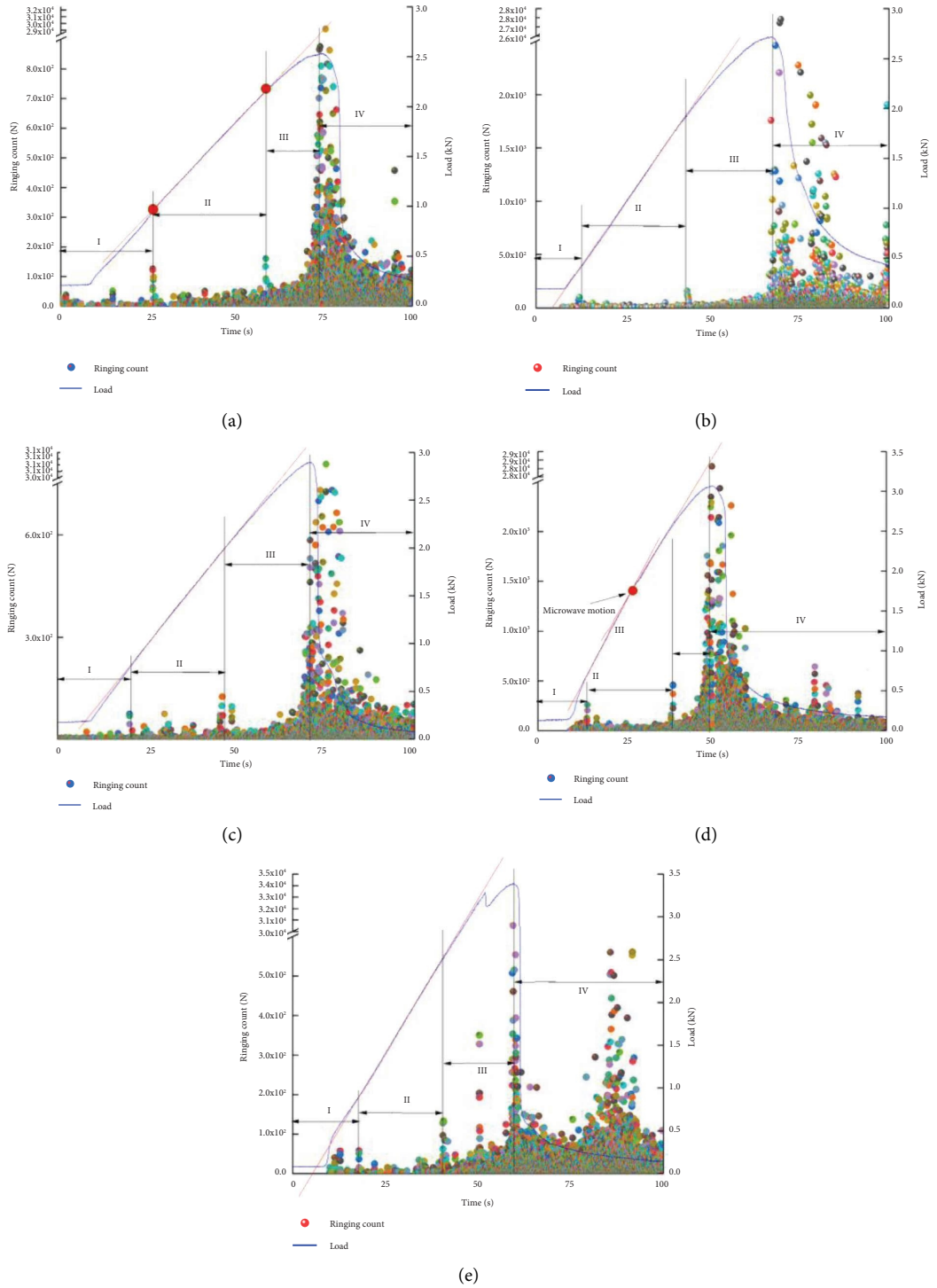

Figure 4: Acoustic emission characteristic parameters and load-time curve of different spans: (a) span 180 mm, (b) span 170 mm, (c) span 160 mm, (d) span 150 mm, and (e) span 140 mm.

the acoustic emission signal is active; the third case is the expansion of local primary cracks under load or has produced newborn cracks, indicating that the specimen has more primary defects or local weak areas, and the smaller load action that the crack sprouting. From the above three cases, we get that the specimen primary state has a significant influence on the crack evolution, and the specimen primary state has a certain randomness. With the increase in span distance, the stage II shows an obvious increasing trend.

The acoustic emission signal enters the active stage in stage III, which is also an important stage for prediction and forecasting. With the increase of load, the acoustic emission ringing count shows obvious accelerated growth, and the acoustic emission ringing count reaches the maximum at the

moment of rupture. This stage contains the expansion of primary microcracks near the rupture zone in the lower part of the neutral layer, the sprouting of new cracks, the penetration of primary cracks, the penetration of newborn cracks and primary cracks, especially at the moment of rupture, the initial fracture in the lower middle has been formed, the high-energy rupture event occurs, and the high ringing counts also appear. Therefore, the arrival of rupture can be judged by the sudden increase in acoustic emission ringing count.

Stage IV is more complicated, including the loss of bearing capacity phase and residual stress phase. By analyzing the crack extension process, it is found that the three-point bending crack penetration is completed under low load, followed by the crack extension period after the peak. Under the load, the crack extension, extension direction, and speed are related to the acoustic emission ringing count. The acoustic emission signal maintains a high amplitude and frequency of ringing counts, according to which also indicates that the sandstone completes the crack extension. The acoustic emission ringing counts in the postpeak residual phase show two situations, one is to keep continuously active (spanning 180 mm, 160 mm, and 150 mm), mainly because the fracture initiation near the lower middle of the sandstone has been formed, and the fracture continues to extend upward under the push of continuous displacement, and the fracture extension speed is relatively smooth; one is aggregation active (spanning 170 mm and 140 mm), and the acoustic emission ringing counts. The high-frequency high count signal occurs again after the active period, indicating that the crack extension is intermittent, and the extension occurs again after the deformation reaches a certain degree. It is found that the acoustic emission ringing count is more active postpeak than prepeak, mainly because of the difference in the intensity and frequency of the elastic wave released by the crack sprouting and expansion.

Figure 5 shows the cumulative acoustic emission ringing counts at the peak of different spans. With the increase of the span, the accumulated acoustic emission ringing counts show a decreasing trend, and the rate of change is gradually decreasing, which indicates that the intensity of rupture is gradually decreasing, but the decay. The rate of change is decreasing, indicating that the intensity of rupture is decreasing, but the decay is getting faster.

4. Analysis of Sandstone Rupture Precursor Information

Prerupture of coal rock leads to obvious acoustic emission phenomenon due to intensive activity of cracks, and this stage is relatively short compared to the prepeak period, so accurate capture and judgment of acoustic information are the key stage of early warning forecasting. In order to explore the precursor information of rock rupture more comprehensively, we analyze the acoustic law of three-point bending sandstone prerupture from the time domain, frequency domain, and ratio of acoustic emission cumulative ringing count to cumulative energy count (R value) and give the rupture warning characteristics in this way.

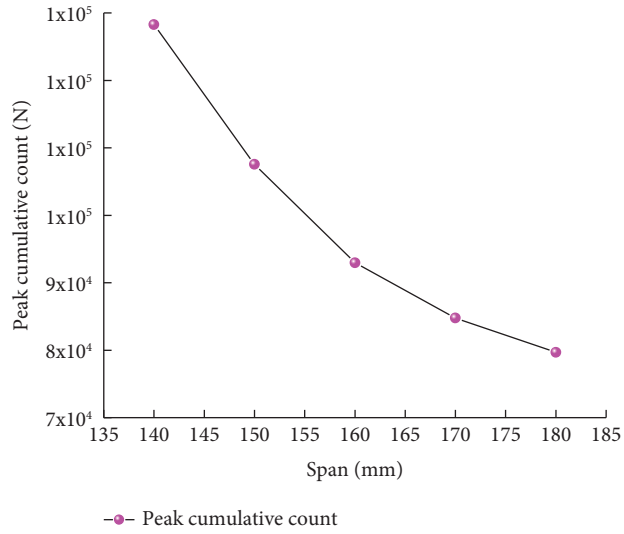

Figure 5: Cumulative ringing count curve of acoustic emission in different spans.

4.1. Time Domain Analysis. From the perspective of time domain precursor information identification, it is crucial to find the acoustic emission ringing count anomaly at the prefracture stage. The whole curve of acoustic emission cumulative ringing count shows a significant and rapid growth in stage II, which needs to be refined and analyzed to dig deeper into the dynamic properties of acoustic emission cumulative ringing count at the prerupture stage, taking the span of 140 mm as an example, as shown in Figure 6.

Initially, there is a sudden jump in growth, indicating that at this time, the rock sample breaking. The first-stage and second-stage slopes are 59 and 134, respectively, and the microcrack extension enters a more stable period; after the linear end point, the accumulated acoustic emission ringing counts show an accelerated growth trend, a virtual circle is drawn with the linear end point as the vertical line, the end point of the arc is the starting point of the accelerated growth, and the acceleration phase calculated by the angle of the acceleration stage is 64.6° by diameter and arc length, and the microcracks converge and coherence at this stage.

The above analysis can be used to predict the sandstone three-point bending rupture by the evolution characteristics of the acoustic emission cumulative ringing count stage II. The initial feedback is the jump growth of acoustic emission ringing count, the secondary feedback is the dividing point of the linear growth of stage II, and the third feedback is the starting point of the arc, whose corresponding percentage of forecast time is 81%, 87%, and 97%, respectively, and the forecast data are evenly distributed and progressive step by step, indicating that the selected characteristic parameters and cutoff points are reliable.

4.2. Frequency Domain Analysis. According to the frequency spectrum law at different crack evolution stages of three-point bending test, the peak frequency shows an increasing trend before the peak point, which can reveal the precursor information of fracture from the perspective of frequency

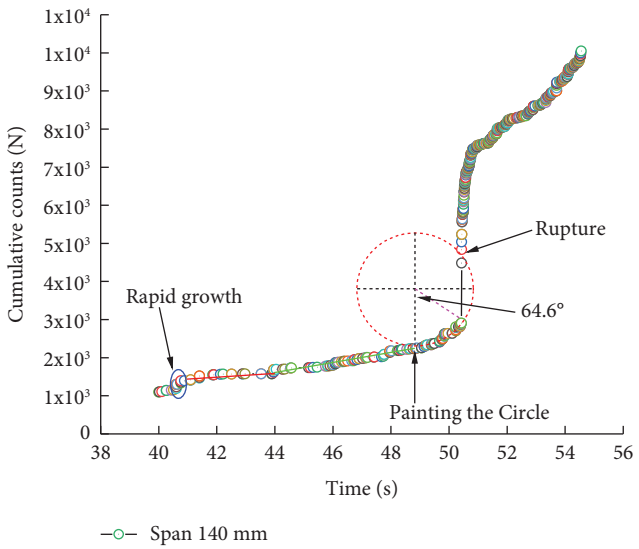

Figure 6: Variation curve of acoustic emission cumulative ringing count in the whole loading process.

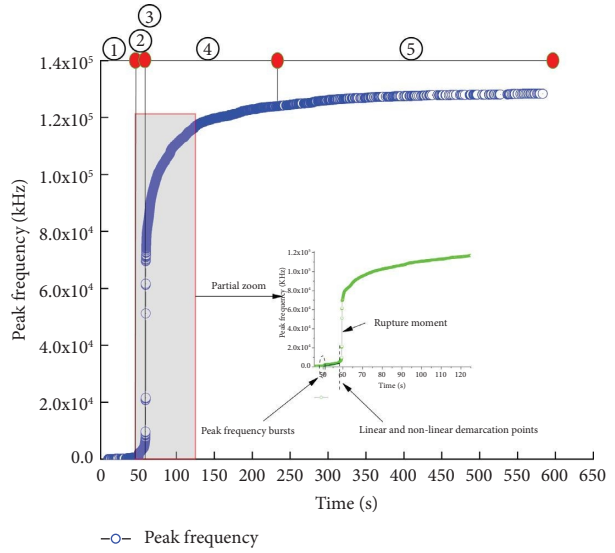

Figure 7: Cumulative peak frequency curve of acoustic emission.

domain. Figure 7 gives the change curve of the accumulated peak frequency of acoustic emission, which can be divided into five stages according to the analysis of its change law, the first stage of low peak frequency and slow growth rate is the microcrack adjustment and budding activity period; the second stage of peak frequency accelerated growth is the crack expansion and penetration period; the third stage of the rapid growth of peak frequency is the crack local penetration period, in the lower part of the specimen to form. The fourth stage of peak frequency deceleration growth is the crack extension period, and the lower part of the specimen cracks gradually to the upper loading line extension; the fifth stage of peak frequency remains stable; at this time, the main control fracture has been formed, three-point bending rupture surface separation process of sandstone rupture zone tear and slip caused by changes. The second and third stages of peak frequency are important intervals for precursor information identification, so it is locally amplified. The analysis found that the peak frequency showed a sudden increase followed by linear growth and then accelerated growth to rupture, and the two characteristic points of peak frequency were obtained as sudden increase and linear and nonlinear demarcation point, whose corresponding percentage of forecast time was 85% and 97%, respectively, indicating that it is reasonable and feasible to forecast rupture from frequency domain perspective.

4.3. Acoustic Emission R Value. Acoustic emission ringing counts characterize the active degree of cracking, and acoustic emission energy characterizes the energy released from the crack source. Using the ratio of cumulative acoustic emission ringing counts and cumulative energy counts defined as the R value [21], the R value can characterize the degree of internal energy concentration, which is given by

$$R = \frac{\sum N}{\sum E}. \tag{1}$$

Figure 8 gives the variation pattern of R value during the loading to fracture of the three-point bending sandstone. The R value remains basically unchanged in the late peak period, indicating that weaker cracking activity occurs after the peak. The R value changes are more drastic in the prepeak period and the early postpeak period, and local amplification analysis is performed for this stage.

The initial loading stage R value shows a sharp increase and then decreasing trend; at this time, the acoustic emission signal experienced a relative low-energy high ringing count and high-energy high ringing count stage; the decrease of R value is not the generation of large fissures, the initial loading energy and ringing count are relatively small, the primary defect adjustment triggered the growth of energy ringing count leads to the decrease of R value, and the initial loading stage R value change law reference value is not significant.

The sudden increase of R value in the middle of loading shows linear growth and one sudden increase, which indicates that the acoustic emission activity is becoming more and more intense, the slope of the curve increases significantly after the sudden increase of R value, the growth rate of acoustic emission energy decreases, and the growth rate of acoustic emission ringing count increases. R value of sudden increase can be used as a precursor feature, and the unstable deformation of the specimen occurs.

The R value decreases and then increases to the peak and then decreases again at the moment of rupture, which also indicates that the R value can characterize the degree of crack expansion and the stage in which it is located. R value decreases indicate that the through crack is breeding the main rupture, so the low point of the R value decreasing process and the high point of the increasing process at this stage can be used as the precursor of rupture.

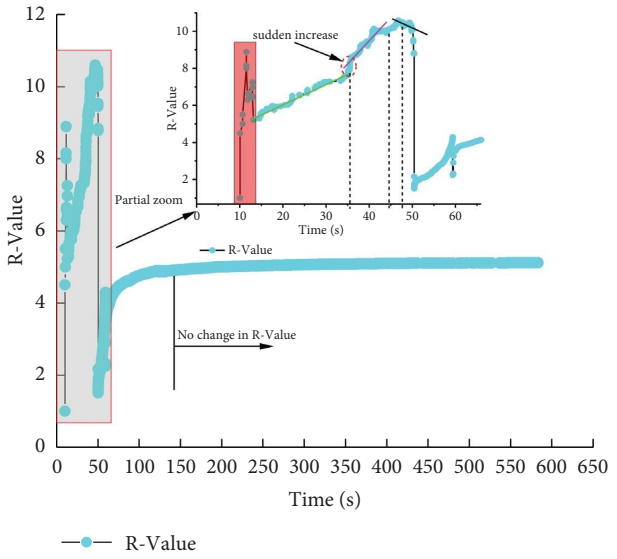

Figure 8: Variation curve of R value in the whole loading process.

5. Analysis of the Damage Evolution Law Characterized by Acoustic Emission Characteristic Parameters

During the sandstone three-point bending experiment, the crack emerges and forms a cracking point, and the crack extends upward from the cracking point to the fracture of the specimen. The sandstone damage evolution process of the three-point bending experiment can be divided into two stages, namely, the damage formation stage and the residual damage stage. Based on the consistency of damage and crack evolution, this section uses acoustic emission characteristic parameters to characterize the damage, analyze the damage evolution law of the whole process of three-point bending damage, and study the damage evolution characteristics of sandstone experimental sandstone with different span three-point bending.

Under the load, the sandstone loading line corresponding to the effective cross-sectional area will decrease, and the equivalent cross-sectional area after fracture is 0. In this way, the concept of damage is proposed [22], namely,

$$D = \frac{A_{\text{orig}} - A_{\text{loss}}}{A_{\text{orig}}}, = 1 - \frac{A_{\text{loss}}}{A_{\text{orig}}}, \tag{2}$$

where D is the damage variable, between 0 and 1, 0 is no damage, 1 is complete fracture; A_{orig} is the longitudinal cross-sectional area of the loading line of the undamaged specimen; A_{loss} is the longitudinal cross-sectional area of the loading line of the damaged specimen.

In the practical application process, the effective area of the longitudinal section of the three-point bending loading line is difficult to determine, and referring to the method proposed in the paper [23] to determine the damage variable through the effective stress, the effective stress can be determined during the single and triaxial experiments, and the stress cannot be calculated for the three-point bending experiments, so the damage variable is determined by the effective load as follows:

$$F' = \frac{F}{1 - D}, \tag{3}$$

where F' is the effective load, and F is load, unit kN.

According to the theory of elastic mechanics, the relationship between the displacement of sandstone and the load and damage variables is obtained as follows:

$$d = \frac{F'}{k}, = \frac{F}{k(1 - D)}, \tag{4}$$

where d is the displacement of the sandstone loading line in mm; k is the elastic constant.

Since the rock particles and cementation components are random, the strength of microunits is also random, and assuming that the microunit strength obeys the Weibull statistical distribution [16].

$$\varphi(a) = \frac{m}{a_0}\left(\frac{a}{a_0}\right)^{m-1} e^{-(a/a_0)^m}, \tag{5}$$

where a is the microelement mechanical parameter, a_0 is the average microelement mechanical parameter, and m is the homogeneity of the sandstone.

Under the action of load, the sandstone particle microelement transforms from the stable state to the unstable state, and the probability density function is the damage rate calculated by counting the unstable state of the microelement, by which the macroscopic damage degree of the specimen can be characterized. Assuming that the number of unstable microelements is n when a certain load is reached, the number of unstable microelements inside the specimen when the displacement increases is, and the number of microelements when the displacement is d is obtained as follows:

$$n(d) = \int_0^d N\phi(x)\mathrm{d}x, = N\left(1 - e^{-(d/a_0)^m}\right). \tag{6}$$

The rock will release strain energy outward during the crack extension process, and the acoustic emission characteristic parameters are consistent with the strain energy [24], and the damage degree of the rock can also be characterized by the acoustic emission characteristic parameters, and the relationship between the damage variable D and the acoustic emission characteristic parameters and statistical microelement changes is given by

$$D = \frac{N_1}{N_m}, = 1 - e^{-(d/a_0)^m}, \tag{7}$$

where N_1 is the cumulative acoustic emission ringing count when the displacement is d, and N_m is the cumulative

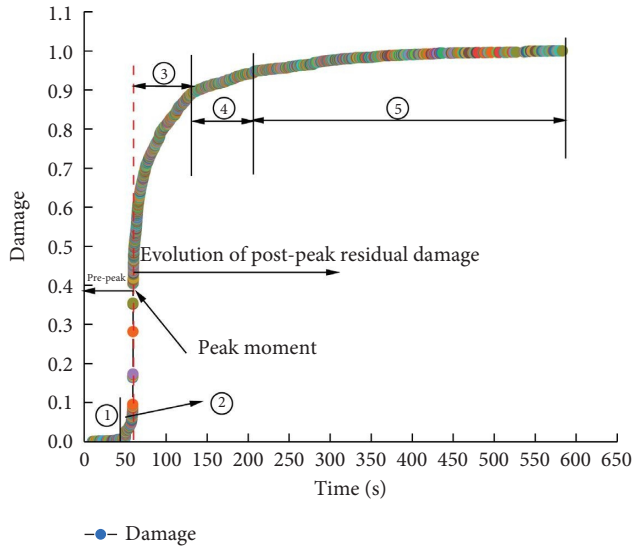

Figure 9: The change law of damage variables characterized by acoustic emission characteristic parameters.

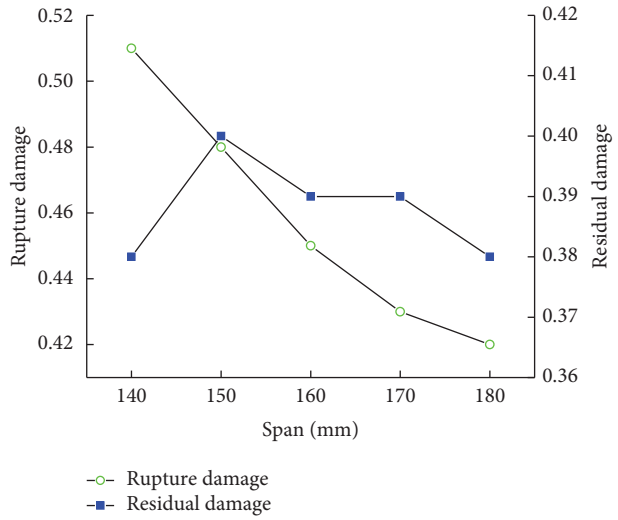

Figure 10: Characteristic analysis of different span damage evolution stages.

acoustic emission ringing count when the sandstone is completely fractured.

The above analysis is based on the fracture of the rock when it reaches the ultimate bearing capacity. The specimen cracked when the peak load was reached in the three-point bending experiment and did not fracture, and the degree of damage was still increasing during the extension and expansion of the crack. According to the characteristics of the three-point bending experiments, the residual damage variable D_t is proposed, and the damage variable expression is

$$D_t = \frac{N_m - N_1}{N_m}. \tag{8}$$

Through the acoustic emission cumulative ringing count and theoretically derived damage formula, the damage characteristics of the specimen parameters are calculated, the damage degree of the peak moment of the specimen is only 0.51, the residual damage variable of the fracture process after cracking reaches 0.49, uniaxial, triaxial, and shear of the experimental peak moment damage are generally above 0.8, and the residual damage of the residual stage after the peak of the three-point bending experiment has the significance of the discussion [25–27].

Specimen damage variable changes pattern, see Figure 9. According to the damage variable, curve characteristics will be divided into five stages, stage I damage is small, the rate of change is smooth and low, it can be considered that this stage of sandstone specimens under the action of the load did not occur damage; stage II damage change rate gradually increased, the damage entered a violent evolutionary stage, this stage formed the initial fracture, the peak moment of load damage variable increased to 0.51, stage III damage rate shows a gradually decreasing trend, the specimen crack occurs relatively stable extension, and this stage damage variable increased by 0.38; stage IV main control crack has penetrated, the sandstone has lost the load-bearing capacity, the specimen completely fractured, and damage variable reached 0.94; stage V is mainly sandstone specimen completely fractured after the slip and friction between the fractured rock blocks.

In order to analyze the damage evolution characteristics of sandstone in three-point bending experiments with different span distances, the curves of rupture damage and residual damage with different span distances were drawn, as shown in Figure 10. With the increase of span distance, the rupture damage showed a decreasing trend; the residual damage fluctuated between 0.38 and 0.40, and the crack extension trajectories were different, but the unfolding lengths were similar, so the residual damage results were similar.

6. Conclusion

Three-point bending experiments were carried out on sandstone samples with different spans using a press and acoustic emission system. AE characteristic parameters, fracture law, and damage evolution law of sandstone were obtained. The main conclusions are as follows:

(1) According to the fluctuation of acoustic emission ringing count, the load-time curve was divided into four typical stages: the first stage showed an increasing trend; the second stage showed an obvious increasing trend. The third stage showed an obvious acceleration of growth, and the acoustic emission ringing count reaches the maximum at the moment of rupture. In the fourth stage, the amplitude and frequency of the ringing count are large and high. With the increase in span, the cumulative ringing counts of AE showed a decreasing trend, and the rate of change gradually decreased.

(2) The failure process of three-point bending sandstone can reflect the precursor information of rock failure from time domain, frequency domain, and R value. In time domain, the evolution characteristics of stage II of acoustic emission cumulative ringing count can

be used to predict the three-point bending fracture of sandstone. The peak frequency shows a linear increase after a spike and then an accelerated increase to a rupture, and the boundary point between the spike and the linear and nonlinear can be obtained. The decrease in R value can indicate that the main crack is growing in the specimen.

(3) According to the damage rate, the damage variable characteristics of the specimen can be divided into five stages: stationary and low, gradually increasing, gradually decreasing, main crack through, and complete fracture. With the increase in span, the fracture damage shows a decreasing trend. The residual damage fluctuates between 0.38 and 0.40 due to the difference in crack propagation trajectory.

Data Availability

The data used to support the study are available within the article.

Conflicts of Interest

The authors declare that they have no conflicts of interest.

Acknowledgments

This study was supported by the Outstanding Young Talents Project of Central Government for the Reform and Development of Local Universities (2020YQ13) and Scientific and Technological Key Project of "Revealing the List and Taking Command" in Heilongjiang Province: Study on Geological Model and Ventilation Model of Intelligent Mining in Extremely Thin Coal Seam (2021ZXJ02A03).

References

[1] T. Li, K. X. Li, X. Y. Pi, and C. Fang, "Time-dependent behavior of acoustic emission feature parameters of sandstone under bending load," *Journal of China Coal Society*, vol. 43, no. 11, pp. 3115–3121, 2018.

[2] H. P. Kang, "Seventy years development and prospects of strata control technologies for coal mine roadways in," *China" Chinese Journal of Rock Mechanics and Engineering*, vol. 40, no. 01, pp. 1–30, 2021.

[3] H. P. Kang, G. Xu, B. M. Wang et al., "Forty years development and prospects of underground coal mining and strata control technologies in China," *Journal of Mining and Strata Control Engineering*, vol. 1, no. 02, pp. 7–39, 2019.

[4] Q. X. Qi, Y. Z. Li, S. K. Zhao et al., "Seventy years development of coal mine rockburst in China: establishment and consideration of theory and technology system," *Coal Science and Technology*, vol. 471, no. 09, pp. 1–40, 2019.

[5] S. J. Chen, Z. H. Zhao, F. Feng, and M. Z. Zhang, "Stress evolution of deep surrounding rock under characteristics of bi-modulus and strength drop," *Journal of Central South University*, vol. 29, no. 2, pp. 680–692, 2022.

[6] C. F. Deng, J. F. Liu, L. Chen, Y. Li, and G. Xiang, "Study on the mechanical behavior and acoustic emission characteristics of fracture of granite with different grain sizes," *Geotechnics*, vol. 37, no. 08, pp. 2313–3232, 2016.

[7] W. C. Zhu, S. L. Wang, and C. A. Tang, "Computer simulation of concrete three-point bending test," *Journal of Northeastern University*, vol. 20, no. 5, pp. 533-534, 1999.

[8] H. P. Xie and Z. H. Chen, *Rock Mechanics*, Science Press, Beijing, China, 2004.

[9] J. P. Zuo, H. W. Zhou, and Y. J. Liu, "Study of characteristic parameters of three-point bending damage of sandstone at different temperatures," *Journal of Rock Mechanics and Engineering*, vol. 29, no. 04, pp. 64–71, 2010.

[10] J. Wei, W. C. Zhu, R. F. Li, L. L. Niu, and Q. Y. Wang, "Experiment of the tensile strength and fracture toughness of rock using notched three point bending test," *Journal of Water Resources and Architectural Engineering*, vol. 14, no. 03, pp. 128–132, 2016.

[11] J. P. Zuo, H. W. Zhou, X. Fan, and Y. Ju, "Research on fracture behavior of BEISHAN granite after heat treatment under three-point bending," *Chinese Journal of Rock Mechanics and Engineering*, vol. 32, no. 12, pp. 2422–2430, 2013.

[12] S. Heng, X. Liu, X. Z. Li, X. D. Zhang, and C. H. Yang, "Study on the fracture propagation mechanisms of shale under tension," *Chinese Journal of Rock Mechanics and Engineering*, vol. 38, no. 10, pp. 2031–2044, 2019.

[13] H. Lu, X. F. Feng, C. X. Yang, and X. W. Zhang, "Effect of different notch prefabrication methods and notch lengths on rock three-point bending test," *Rock and Soil Mechanics*, vol. 42, no. 04, pp. 1115–1125, 2021.

[14] K. Zhao, Y. T. Zhou, P. Zeng, and C. Y. Lu, "Experimental study on acoustic emission characteristics of rock-like materials with different particle sizes under three-point bending," *Journal of China Coal Society*, vol. 43, no. 11, pp. 3107–3114, 2018.

[15] D. X. Yang, "Acoustic emission behavior characteristics of rock micro-fracture evolution based on deep learning," *Chinese Journal of Rock Mechanics and Engineering*, vol. 41, no. 8, p. 1728, 2022.

[16] C. L. Wang, C. Cao, C. F. Li, X. S. Chuai, G. M. Zhao, and H. Lu, "Experimental investigation on synergetic prediction of granite rockburst using rock failure time and acoustic emission energy," *Journal of Central South University*, vol. 29, no. 4, pp. 1262–1273, 2022.

[17] X. L. L Z. Liu, X. B. Li, M. S. Han, and L. Q. Yang, "Acoustic emission and micro-rupture characteristics of rocks under Brazilian splitting load," *Chinese Journal of Engineering*, vol. 41, no. 11, pp. 1422–1432, 2019.

[18] X. L. Li, S. J. Chen, S. M. Liu, and Z. H. Li, "AE waveform characteristics of rock mass under uniaxial loading based on Hilbert-Huang transform," *Journal of Central South University*, vol. 28, no. 6, pp. 1843–1856, 2021.

[19] R. Yang, L. Jiakun, B. Zhou, and D. P. Ma, "Rock unloading failure precursor based on acoustic emission parametric fractal characteristics," *Lithosphere*, vol. 2022, Article ID 8221614, 2022.

[20] W. G. Han, Z. D. Cui, T. W. Tang, J. Y. Zhang, and Y. Z. Wang, "Effects of different bedding plane strength on crack propagation process under three points bending," *Journal of China Coal Society*, vol. 44, no. 10, pp. 3022–3030, 2019.

[21] G. Liu, Y. M. Li, F. K. Xiao, S. J. Huang, and R. F. Zhang, "Study on failure mechanics behavior and damage evolution law of yellow sandstone under uniaxial triaxial and pore water action," *Chinese Journal of Rock Mechanics and Engineering*, vol. 38, no. S2, pp. 3532–3544, 2019.

[22] C. B. Li, H. P. Xie, and L. Z. Xie, "Experimental and theoretical study on the shale crack initiation stress and crack damage

stress," *Journal of China Coal Society*, vol. 42, no. 4, pp. 969–976, 2017.

[23] X. R. Wang, E. Y. Wang, F. Liu, X. L. Li, H. Wang, and D. X. Li, "Macro-crack propagation process and corresponding AE behaviors of fractured sandstone under different loading rates," *Chinese Journal of Rock Mechanics and Engineering*, vol. 37, no. 6, pp. 1446–1458, 2018.

[24] Y. N. Rabotnov, "On the equation of state of creep," *Proceedings of the Institution of Mechanical Engineers, Conference Porceedings*, vol. 178, no. 1, pp. 2117–2122, 1963.

[25] J. Lemaitre, "A continuous damage mechanics model for ductile fracture," *Journal of Engineering Materials and Technology*, vol. 107, no. 1, pp. 83–89, 1985.

[26] C. A. Tang, S. L. Wang, and Y. F. Fu, *Numerical Experiments on Rock Fracture Process*, Science Press, Beijing, China, 2003.

[27] K. Zhao, J. F. Jin, X. J. Wang, and K. Zhao, "Study on the relationship between sound velocity of rock and its damage and acoustic emission," *Geotechnical Mechanics*, vol. 28, no. 10, pp. 2105–2109, 2007.